Pair Production as a Probe of Colliding Beam Size *

Pisin Chen, John Irwin, and Anatoly Spitkovsky
Stanford Linear Accelerator Center
Stanford University, Stanford, CA 94309, USA

Abstract

We propose the use of soft e^+e^- pairs as a non-evasive measurement of the colliding beam size. The angular distribution of the pair particles that have different sign of charge from that of the opposing beam, provides the information about the aspect ratio of the beam. The transverse momentum of the other species in the pair, on the other hand, carries information about the horizontal dimension of the beam. Together, one can in principle measure both σ_x and σ_y.

1 INTRODUCTION

The sizes of the colliding beams in the next generation of linear colliders are expected to be in the nanometer range. This poses a great challenge to the monitoring of the beams and the tuning of the machine. Conventional monitors fail below the micrometer range, so alternative approach is clearly needed. Several novel concepts have been proposed in recent years[1, 2, 3]. The initial experimental tests of these approaches at SLAC's Final Focus Test Beam (FFTB) have been very successful. Nevertheless, considering excessive hardware necessary for these devices, it is still desirable to find a solution which requires minimal hardware around the interaction point (IP), and is non-evasive to the beam monitored. In this paper we propose the concept of measuring the beam size by monitoring the soft e^+e^- pairs produced during beam-beam interaction which are subsequently deflected by the beam field.

We know that beamstrahlung photons can turn into e^+e^- pairs. At lower energies, these pairs will be deflected by the beam field more strongly than the primary high-energy particles. This helps to separate them from the primary particles for signal collection. Furthermore, the bulk of these pairs, although been kicked more strongly, still has an outcoming angle which is smaller than the detector masking angle. This allows one to position the monitor downstream from the IP. The situation, nontheless, is complicated by the drift through the solenoidal field in the detector. With such a field included in our analysis, we demonstrate that clear signals on the beam size can be obtained in this approach.

*A preliminary account of this idea was presented at the LC93 Workshop, SLAC, Stanford, Nov. 1993;
Work supported by Department of Energy contract DE-AC03-76SF00515.

2 PAIR PRODUCTION

There are two main types of pair production processes during the beam-beam interaction: Either under the influence of the collective electromagnetic field of the beam (coherent)[4]; or through the standard two-body interaction processes (incoherent). Since essentially all the designs of the next generation linear colliders have the beamstrahlung parameter $\Upsilon = 2\gamma B/B_c$ (where B is the average electromagnetic field strength of the beam and $B_c = m^2c^3/e\hbar \simeq 4.4 \times 10^{13}$G is the Schwinger critical field) smaller than the threshold value of 0.3 for coherent pair creation, we can ignore the contribution of the coherent pairs. Then all the pairs that we consider are from the incoherent processes. There are three incoherent processes in this context: the Breit-Wheeler (BW) process: $\gamma\gamma \to e^+e^-$; the Bethe-Heitler(BH) process: $e^\pm\gamma \to e^\pm e^+e^-$; and the Landau-Lifshits(LL) process: $e^+e^- \to e^+e^-e^+e^-$. Since all three processes involve the basic kernel $\gamma\gamma \to e^+e^-$, where γ can be either real (beamstrahlung) or virtual, one can calculate the cross-sections by using the equivalent photon approximations. A detailed analysis of this problem can be found in [5]. The total cross-sections are

$$\sigma_{BW} = \frac{3}{8}(\ln 4 + \frac{3}{2})\pi r_e^2 \gamma_\circ^{-\frac{2}{3}}(L - \ln 4)A^2, \quad (1)$$

$$\sigma_{BH} = \frac{28}{3}\alpha r_e^2 (L - \frac{234}{42})A, \quad (2)$$

$$\sigma_{LL} = \frac{\alpha^2 r_e^2}{\pi}(\frac{28}{27}L^3 - 6.59L^2 - 11.8L + 104), \quad (3)$$

where $r_e = e^2/mc^2$, $A = (\Gamma(2/3)/\pi)(\alpha\sigma_z/\gamma_\circ\lambda_c)(3\Upsilon)^{2/3}$ and $L = \ln 4\gamma_\circ^2$. $\gamma_\circ$ is the Lorentz factor of the primary beam particles. For NLC, the beam energy is 250 GeV, $\Upsilon \simeq 0.1$, $N = 6.5 \times 10^9$, and $\sigma_z = 100\mu$m, and the total number of pairs is expected to be of the order of a million. The contributions are not the same, however, among the three processes. In general, $\sigma_{BH} > \sigma_{LL} \gg \sigma_{BW}$. For instance, for NLC parameters we have $\sigma_{BH} : \sigma_{LL} : \sigma_{BW} \sim 150 : 30 : 1$. It is therefore sufficient to only consider pairs generated by the BH process in our following analysis. Since the beamstrahlung photons are more abundant around the maximum beam filed, the BH pairs are densely populated around the edge of the beam cross section.

3 DISRUPTION OF SOFT PAIRS

The motion of pairs in the beam is determined by the EM field of the Gaussian bunch. The nature of the field is

such that forces on the particle in both x (horizontal) and y (vertical) directions experience a linear rise from zero value at the center to some maximum and then decay to zero at infinity. If a particle has charge opposite to that of the oncoming beam, the field of the beam creates a potential well inside which the particle oscillates. In the linear approximation one can find the maximum deflection angles in x and y directions[9]:

$$\theta_{x,y}^{max} \sim \frac{\theta_0}{\sqrt{\sqrt{3}uD_{x,y}}}, \quad D_{x,y}/u \gtrsim 1/\sqrt{3}, \tag{4}$$

where u is particle's fractional energy, $\theta_0 = D_{x,y}\sigma_{x,y}/\sigma_z$, and $D_{x,y} = 2Nr_e\sigma_z/[\gamma_0\sigma_{x,y}(\sigma_x+\sigma_y)]$ is the disruption parameter for the primary particles. Therefore, the outcoming particles of this species has a preferential angle which is proportional to $\theta_x/\theta_y \sim \sqrt{D_y/D_x} = \sqrt{R}$, i.e., it is peaked around the horizontal axis. The full-width-half-maximum (FWHM) of this distribution is, therefore, dependent on aspect ratio of the beam, and scales as $1/\sqrt{R}$ (fig.1).

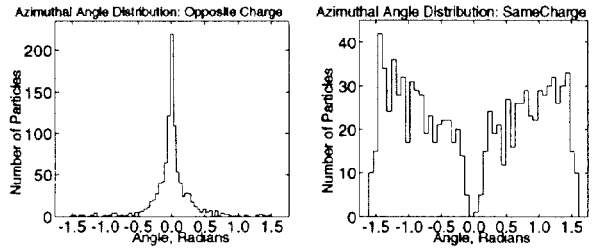

Figure 1. Azimuthal angular distributions for opposite and same charge

In order to measure the beam size in both dimensions, additional information on one of the dimensions (σ_x or σ_y) is needed. It turns out that the other species of particles in the pair that has the same sign of charge as the oncoming beam can provide information on σ_x. These particles experience repulsive force as they traverse through the beam. Kicked by the beam, they acquire transverse momentum considerably greater then their inherent transverse momentum. Maximum gain in transverse momentum, i.e., momentum gained by a "heavy" particle riding on the peak of the field during beam passage, can be obtained as [6]:

$$\Delta p_{x_m} = \frac{\sqrt{2}}{0.924}\frac{e^2N}{c\sigma_x}\left[1 - \frac{0.639}{R}\right], \tag{5}$$

$$\Delta p_{y_m} = \sqrt{2\pi}\frac{e^2N}{c\sigma_x}\left[1 - \frac{1+\pi/2}{R\sqrt{\pi\log R}}\right]. \tag{6}$$

Therefore, the transverse momentum of the defelected particles has a clear $1/\sigma_x$ dependence at large R. However, this scaling was confirmed by computer simulations only for particles of considerably high energy, i.e. "heavy" enough to hold on to the maximum of the field without significant transverse displacement. For much lower energies transverse momentum changes linearly with σ_x.

4 DRIFT IN SOLENOIDAL FIELD

As we have shown above, we need to measure angular distribution of the opposite charges and transverse momentum of the same charges in the low energy pairs. This is not a very straightforward task due to the presence of the detector solenoidal magnetic field, which further affects the motion of the low-energy pairs. In the current design of NLC, the beams collide at an angle $\theta_c \sim 40$mrad, and the solenoidal field is pointing to the middle of the two beam lines. We adopt this geometry in the following discussion. Suppose η is the original exit angle of the particle as seen from the direction of magnetic field. Then the perpendicular component of particle momentum is [8]:

$$p_\perp = \eta p_{\rm tot} = \eta u p_\circ, \tag{7}$$

where $p_\circ$ is primary beam momentum. The Larmor radius in this case is:

$$\rho = \frac{p_\perp}{qB} = \eta u\frac{p_\circ}{qB} = \eta u\rho_\circ. \tag{8}$$

Let the distance from the IP to the quad face along the B-filed be L^*, which is typically of the order of a meter, then the arc length on the helix is ηL^*. Therefore, the angle of rotation on the helix is (see figure 2):

$$\Phi = \frac{\eta L^*}{\rho} = \frac{L^*}{u\rho_\circ} \equiv 2\mu. \tag{9}$$

Note that angles Φ and μ depend only on the energy of the particle and not on the initial exit angle. Now we can find the radius-vector from the origin to point A. It is just the length of the chord, which is $2\rho\sin\mu$, or after substituting the expression for ρ, $AB = (\eta L^*)\sin\mu/\mu$. This gives us a mapping of the polar coordinates of a particle moving with and without the solenoidal filed:

$$(r,\theta) \to (r',\theta') \equiv (r\frac{\sin\mu}{\mu}, \theta+\mu). \tag{10}$$

Basically, this mapping involves rotation by an angle μ and a contraction of the radius by a factor $\sin\mu/\mu$. Since μ depends on fractional energy of the particle, particles of different energies will be rotated by different amounts: particles of lower energies will rotate more than higher energy ones.

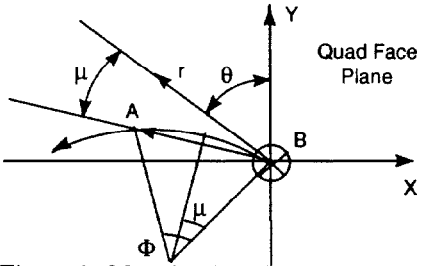

Figure 2. Mapping in solenoidal field

5 SIGNAL EXTRACTION

The solenoidal field discussed above introduces a smearing of the distribution. Nevertheless, Eq.(10) shows that the mapping is a clear function of the pair particle energy. Thus by properly arranging narrow radial and circular slits, and measuring the energy spectrum of the particles that pass through the slits, one should be able to translate

back to the original (r, θ) distributions of the pairs, and thus the beam size. The configuration of such slits differs for opposite and same charge particles (fig.3).

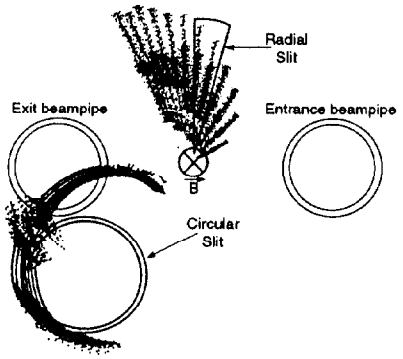

Figure 3. Slits for signal extraction; only half of the "peanut" is plotted.

5.1 Opposite Charge

Since these particles are deflected essentially in the horizontal direction, they come out from IP primarily in the $x - z$ plane, with a "thickness" which is proportional to $1/\sqrt{R}$. This "pancake" is further rotated by the solenoidal field and lands on the quad face around the angle $\theta + \mu$. Imagine a radial slit is cut at this angle, say of 10° span and 3 cm long, with the two edges corresponding to energies E_a and E_b. If the pair particles were monoenergetic and $E_a > E > E_b$, then all particles would pass through this slit. But because the particles have a wide range of energy, only the particles with energies within the range (E_a, E_b) may pass through the slit if the original "pancake" is infinitely thin. Having a finite initial width, however, allows particles with energies slightly above E_a and slightly below E_b to enter the slit. The FWHM of the spectrum tail beyond the energy window (E_a, E_b) therefore reveals the thickness of the initial spot, and thus the aspect ratio R. A typical energy spectrum and the FWHM energy vs. R is shown on fig. 4 (in simulation we use 1000 particles per 0.5 MeV energy bin).

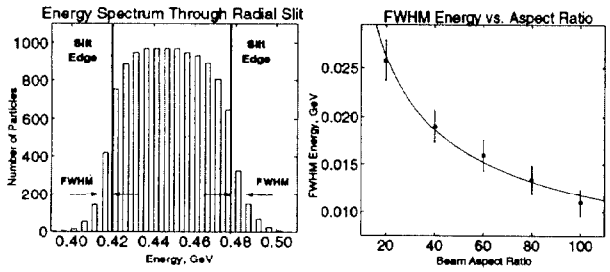

Figure 4. Slit spectrum and R dependence of opposite charge.

5.2 Same Charge

The spatial distribution of the same charge particles is different. Being low in energy, they are able to survey through the entire beam potential, which, when integrated to infinity, is roughly identical in all directions (slightly smaller in horizontal direction). Thus the outcoming spatial distribution of these particles is essentially a cone around the beam with a "peanut" shaped cross section. Their exit angle out of the beam can be written as

$$\tan\alpha = \frac{p_\perp}{p_{||}} = \frac{p_\perp c}{E}. \qquad (11)$$

The solenoidal field does further rotate and distort this peanut shaped distribution. But its geometry is reasonably preserved (see fig.3). We therefore propose to use a circular slit $\sim$ 2cm in diameter positioned below the exit beampipe where the same-sign charges land. Figure 5 shows a typical sampling of the registered energy spectrum through such a slit. As σ_x increases, the angle α and, therefore, the radius of the distribution decrease, and the slit registers higher energies. The plot on the right in fig.5 shows clearly such a dependence.

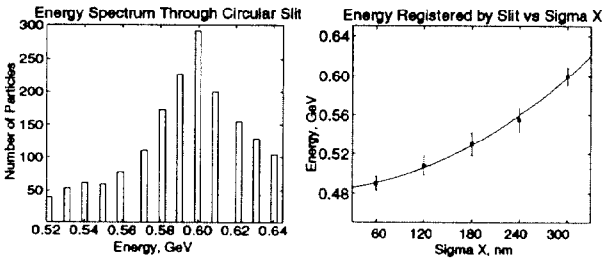

Figure 5. Slit spectrum and σ_x dependence of same charge

6 CONCLUSION

We have shown that soft pairs produced during beam-beam interaction provide the information on both vertical and horizontal beam sizes. We further demonstrate how the information can be extracted downstream from the IP, with the influence of the solenoidal field included. The simulations accounted for only one bunch crossing. The statistics can be much improved when the signals from the whole bunch train are included.

7 REFERENCES

[1] P. Chen, et al., SLAC-AAS-41 (1988); and in the Proc. *Int. Linear Collider Workshop*, SLAC-Report-335, 1988.

[2] J. Buon *et al. NIM* **A306** (1991) 93.

[3] T. Shintake, *NIM* **A311** (1992) 453.

[4] P. Chen and V. Telnov, Phys. Rev. Lett. **63** (1989), 1726.

[5] T. Tauchi, K. Yokoya, P. Chen, *Part. Accel.* **41** (1993) 29.

[6] P. Chen, SLAC-PUB-4923, 1989; and in *Nonlinear and Relativistic Effects in Plasmas*, ed. V. Stefan, AIP Proc. 1992.

[7] M. Bassetti and G.A Erskine, CERN-ISR-TH/80-06,1980.

[8] J. Irwin, "Discussion of crossing angle determination", lecture notes, 1989

[9] K. Yokoya and P. Chen, in *Frontiers of Particle Beam: Intensity Limitations*, ed. M. Dienes, M. Month, and S. Turner, Lect. Notes Phys. 400, Springer-Verlag, 1992.